J Physiol 587.16 (2009) pp 4063–4075

Caffeine inhibition of ionotropic glycine receptors

Lei Duan, Jaeyoung Yang and Malcolm M. Slaughter

Center for Neuroscience and the Department of Physiology and Biophysics, University at Buffalo, SUNY, Buffalo, NY 14214, USA

We found that caffeine is a structural analogue of strychnine and a competitive antagonist at ionotropic glycine receptors (GlyRs). Docking simulations indicate that caffeine and strychnine may bind to similar sites at the GlyR. The R131A GlyR mutation, which reduces strychnine antagonism without suppressing activation by glycine, also reduces caffeine antagonism. GlyR subtypes have differing caffeine sensitivity. Tested against the EC_{50} of each GlyR subtype, the order of caffeine potency (IC_{50}) is: $\alpha2\beta$ ($248 \pm 32\ \mu M$) $\approx \alpha3\beta$ ($255 \pm 16\ \mu M$) $> \alpha4\beta$ ($517 \pm 50\ \mu M$) $> \alpha1\beta$($837 \pm 132\ \mu M$). However, because the $\alpha3\beta$ GlyR is more than 3-fold less sensitive to glycine than any of the other GlyR subtypes, this receptor is most effectively blocked by caffeine. The glycine dose–response curves and the effects of caffeine indicate that amphibian retinal ganglion cells do not express a plethora of GlyR subtypes and are dominated by the $\alpha1\beta$ GlyR. Comparing the effects of caffeine on glycinergic spontaneous and evoked IPSCs indicates that evoked release elevates the glycine concentration at some synapses whereas summation elicits evoked IPSCs at other synapses. Caffeine serves to identify the pharmacophore of strychnine and produces near-complete inhibition of glycine receptors at concentrations commonly employed to stimulate ryanodine receptors.

(Received 1 May 2009; accepted after revision 24 June 2009; first published online 29 June 2009)

Corresponding author L. Duan: Center for Neuroscience, 124 Sherman Hall, University at Buffalo, Buffalo, NY 14214, USA. Email: leiduan@buffalo.edu

Abbreviations BAPTA, 1,2-*bis*(o-aminophenoxy)ethane-*N*,*N*,*N*′,*N*′-tetraacetic acid; GlyR, glycine receptor; IBMX, isobutylmethylxanthine; STR, strychnine

The inhibitory glycine receptor (GlyR), a member of the cysteine-loop superfamily of ionotropic receptors, forms a ligand-gated chloride channel. The receptors are heteromeric pentamers; the native GlyR is formed from two α and three β subunits (Grudzinska *et al.* 2005). In heterologous expression, the α subunits are necessary and sufficient to form functional channels. The β subunits anchor the receptor to the cytoskeleton by interacting with gephyrin (Meyer *et al.* 1995; Kneussel & Betz, 2000) and play a role in glycine binding (Grudzinska *et al.* 2005). There are four genes known that encode α subunits (Matzenbach *et al.* 1994; Laube *et al.* 2002) and one that encodes the β subunit.

Glycine receptors are critical elements in shaping the light signalling pathways in the retina (Wassle, 2004). The retina may be unique in that it expresses all four α subunits (Greferath *et al.* 1994; Haverkamp *et al.* 2003; Heinze *et al.* 2007). Their distributions overlap but are not congruent (Smiley & Yazulla, 1990; Grunert & Wassle, 1996; Sassoe-Pognetto & Wassle, 1997; Haverkamp *et al.* 2004; Jusuf *et al.* 2005; Heinze *et al.* 2007). Each type of retinal GlyR ($\alpha1\beta$, $\alpha2\beta$, $\alpha3\beta$, $\alpha4\beta$) has a distinct expression pattern and postsynaptic response kinetics (Han *et al.* 1997; Gisselmann *et al.* 2002), implying specific functional roles (Ivanova *et al.* 2006). For example, the fast responding, large A-type ganglion cells in mouse retina are dominated by $\alpha1\beta$ GlyRs with fast deactivation kinetics (Majumdar *et al.* 2007).

The development of glycine antagonists could facilitate understanding of GlyR function. At present, there are a few antagonists that show modest selective inhibition of $\alpha2$ *vs.* $\alpha1$ GlyRs (Enz & Bormann, 1995; Han *et al.* 2004; Wang & Slaughter, 2005). However, the pharmacology of GlyRs is rudimentary compared to that of the other members of the receptor superfamily, such as acetylcholine, GABA or serotonin receptors.

To discover novel glycine antagonists, we used the well-know GlyR antagonist, strychnine, as a template and employed analogous, conformationally restricted molecules that might provide insights on the ligand pharmacophore. Strychnine is a very potent, competitive GlyR antagonist (Young & Snyder, 1973). The binding of strychnine at the GlyR ligand binding domain has been extensively studied and mutational analysis indicates that strychnine binding determinants on GlyR overlap with those of glycine, although they are not identical (Marvizon

DOI: 10.1113/jphysiol.2009.174797

et al. 1986; Ruiz-Gomez *et al.* 1990; Rajendra & Schofield, 1995; Grudzinska *et al.* 2005). One outcome of our search is caffeine, a very planar molecule commonly used to inhibit adenosine and stimulate ryanodine receptors. Caffeine is a weak competitive glycine antagonist, with slightly differing IC_{50}s at the four GlyR subtypes. It effectively suppresses glycinergic IPSCs in ganglion cells at low millimolar concentrations.

Methods

Sybyl software (Tripos) was used to compare caffeine and strychnine structures. Both molecules were constructed using Sybyl and underwent Tripos field energy minimization. The nitrogens were not protonated in the model, although they might be in normal physiological solution. Atomic charges were calculated using Gasteiger and Marsili methods. Molecular electrostatic potential and hydrogen bonding maps were displayed on respective Fast Connolly surfaces. Hydrogen donor/acceptors were determined using the Sybyl line notation (SLN) method. Alignment of both molecules was completed by the Sybyl MATCH function, and was based on minimizing the distance between three designated pairs of atoms.

Homology models of the α1 GlyR subunit were made by using the SWISS-MODEL server (Arnold *et al.* 2006). The N-terminal domain sequence of the α1 GlyR was adopted from studies by Speranskiy *et al.* (2007). The nicotoinic acetylcholine receptor (nAChR) (PDB ID: 2BG9) was chosen for the homology modelling using the template identification tool of the SWISS-MODEL server. The sequence alignment between the nAChR and the N-terminal domain of the α1 GlyR was done by the NIH Deepview program. Adding hydrogens and energy minimization were performed by the UCSF Chimera program (Pettersen *et al.* 2004). Two α1 monomers of the glycine receptor were aligned into the nAChR model with structure alignment to form a GlyR dimer. A single amino acid mutation of the model was performed with the mutation tool offered in DeepView (Guex & Peitsch, 1997).

Strychnine and caffeine antagonist docking to the putative binding pocket of the protein was performed using the Autodock 3.0.5 program, as previously described (Speranskiy *et al.* 2007). The protein coordinates were fixed during docking simulations, while the ligands were flexible and moved on the grid as implemented in Autodock. An initial population of 300 starting structures was used for energy optimization with a maximum number of energy evaluations set to 106. The grid spacing was 0.375 Å. All other parameters remained at program default values. Grid searching was performed using the Lamarckian genetic algorithm. Different docking runs were performed to find the best conformation and orientation of ligand, based on the binding energy. The best result was visualized and labelled with the Chimera program.

HEK293 cell lines (American type Culture Collection, VA, USA) were plated on glass coverslips in 35 mm culture dishes for 24 h before transfection. Plasmid DNA containing GlyR α subunit cDNA (in the presence or absence of β subunit cDNA) was added to culture dishes together with FuGENE-6 transfection reagent (Roche Diagnostics Corporation, IN, USA). Cells were cotransfected with EGFP. With a 10 : 1 ratio of GlyR : GFP, a total of 0.22 μg DNA was used for each 35 mm dish. A 1 : 10 ratio of α to β subunit cDNA was used in making $\alpha\beta$ heteromers to avoid homomeric αGlyR formation. Transfected cells were selected based on the presence of green fluorescence.

Larval salamander were stunned, decapitated and enucleated. The retina was then dissected from the eyecup and immediately immersed in amphibian Ringer solution for slicing (Awatramani *et al.* 2001). Handling of animals was in accordance with NIH guidelines and the Animal Care Guidelines of the State University of New York. Retinal ganglion cells were identified based on their cell body location in the ganglion cell layer and large voltage-gated sodium currents.

Whole cell voltage clamp recordings were performed using the Multiclamp 700B amplifier and Clampex9.2 software (Axon Instruments, Foster City, CA, USA). Pipette resistance was usually around 5 MΩ; access resistance was usually around 15–20 MΩ. Retinal slices were superfused with amphibian Ringer solution containing (in mM): 111 NaCl, 2.5 KCl, 1.8 $CaCl_2$ 1 $MgCl_2$, 10 glucose and 5 Hepes, buffered to 7.8 with NaOH. The recording pipette was filled with an internal solution containing (in mM): 100 potassium gluconate, 5 NaCl, 1 $MgCl_2$, 5 EGTA, 5 Hepes and adjusted to pH 7.4 with KOH. The HEK cells were bathed in Krebs solution containing (in mM): 140 NaCl, 4.7 KCl, 1.2 $MgCl_2$, 2.5 $CaCl_2$, 10 Hepes and 10 glucose adjusted to pH 7.4 with NaOH. The pipette solution contained (in mM): 140 KCl, 5.4 NaCl, 2.0 $MgCl_2$, 1.0 $CaCl_2$, 11 EGTA, and 10 Hepes adjusted to pH 7.4 with KOH.

Drugs were delivered through a DAD-12 superfusion system (ALA scientific Instruments Inc., New York, NY, USA). Background superfusion of control Ringer solution was suspended only when the drug was delivered. Glycine, caffeine, theophylline, theobromine, SR95531, IBMX and strychnine were obtained from Sigma (St Louis, MO, USA). Ryanodine was purchased from Tocris (Ellisville, MO, USA). BAPTA was purchased from Calbiochem (La Jolla, CA, USA).

The retina slices were usually light adapted and recorded under normal laboratory light conditions. For recordings of light-evoked IPSCs or EPSCs, the retinal slices were dark adapted for a few minutes before and then during the

recording. Full field red LED light stimuli (660 nm) were employed.

The data were analysed using Clampfit 9.2 (Axon Instruments) and statistical analysis and regression fits were performed using Origin 7.0 (Origin Lab, MA, USA), Igor Pro 5.03 (WaveMetrics Inc., Portland, OR, USA) and Mini Analysis (Synaptosoft Inc., NJ, USA). Antagonists were evaluated by comparing effects of various concentrations of antagonists against fixed concentrations of glycine. In most experiments, the EC_{50} of glycine for each GlyR subtype was used. Inhibitory dose–response curves were fitted with the Hill equation:

$$\frac{I}{I_{\max}} = \frac{1}{1 + \left(\frac{\text{Antagonist}}{[\text{IC}_{50}]}\right)^{n}},$$

where I is the current recorded in the presence of a variable concentration of antagonist [Antagonist]; $I_{\max}$ is the current obtained with a certain concentration of agonist only; EC_{50} and IC_{50} are the concentrations at which the agonist and antagonist produced half maximal response, respectively; and n is the Hill coefficient. Data points are expressed as mean ± S.E.M. (standard error of the mean) with the error bars representing S.E.M.

Results

Caffeine suppressed glycine-activated currents in retinal ganglion cells

Caffeine inhibited activation of GlyRs. This was examined by measuring whole cell currents in neurons from the

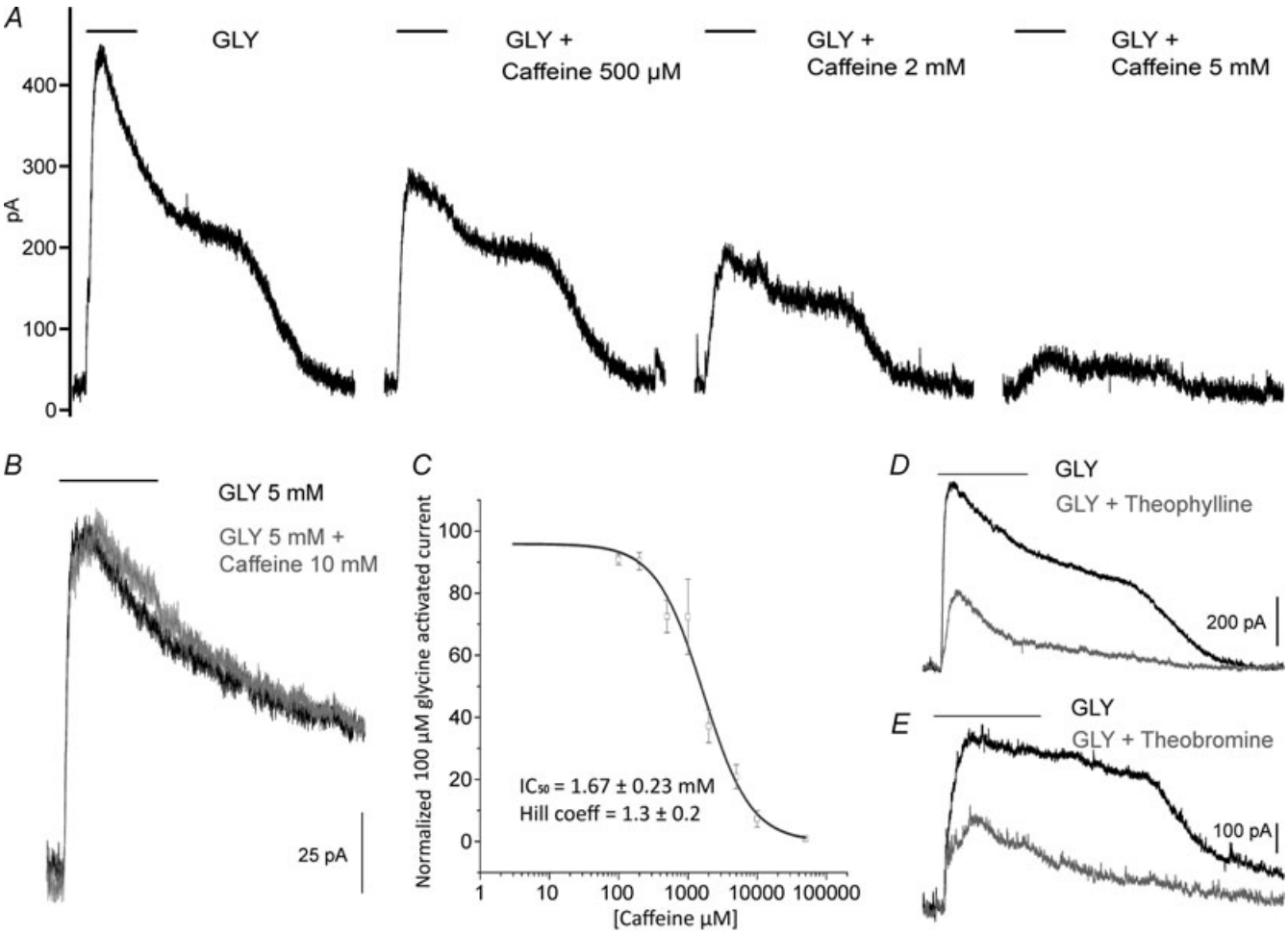

Figure 1. Caffeine suppresses exogenous glycine-activated current on retinal ganglion cells (RGCs)
A, caffeine suppressed the response to 100 μM glycine (dark bars above current traces) in a retinal ganglion cell in a dose-dependent manner. *B*, 5 mM glycine overcame the caffeine block. *C*, dose–response curve of caffeine suppression of 100 μM glycine-activated current (IC_{50} = 1.67 ± 0.23 mM, Hill coefficient = 1.3 ± 0.2, n = 9). *D* and *E*, the currents produced by100 μM glycine were inhibited by 2 mM theophylline (*D*) or 2 mM theobromine (*E*). Ganglion cells in the retinal slice preparation were voltage clamped at 0 mV.

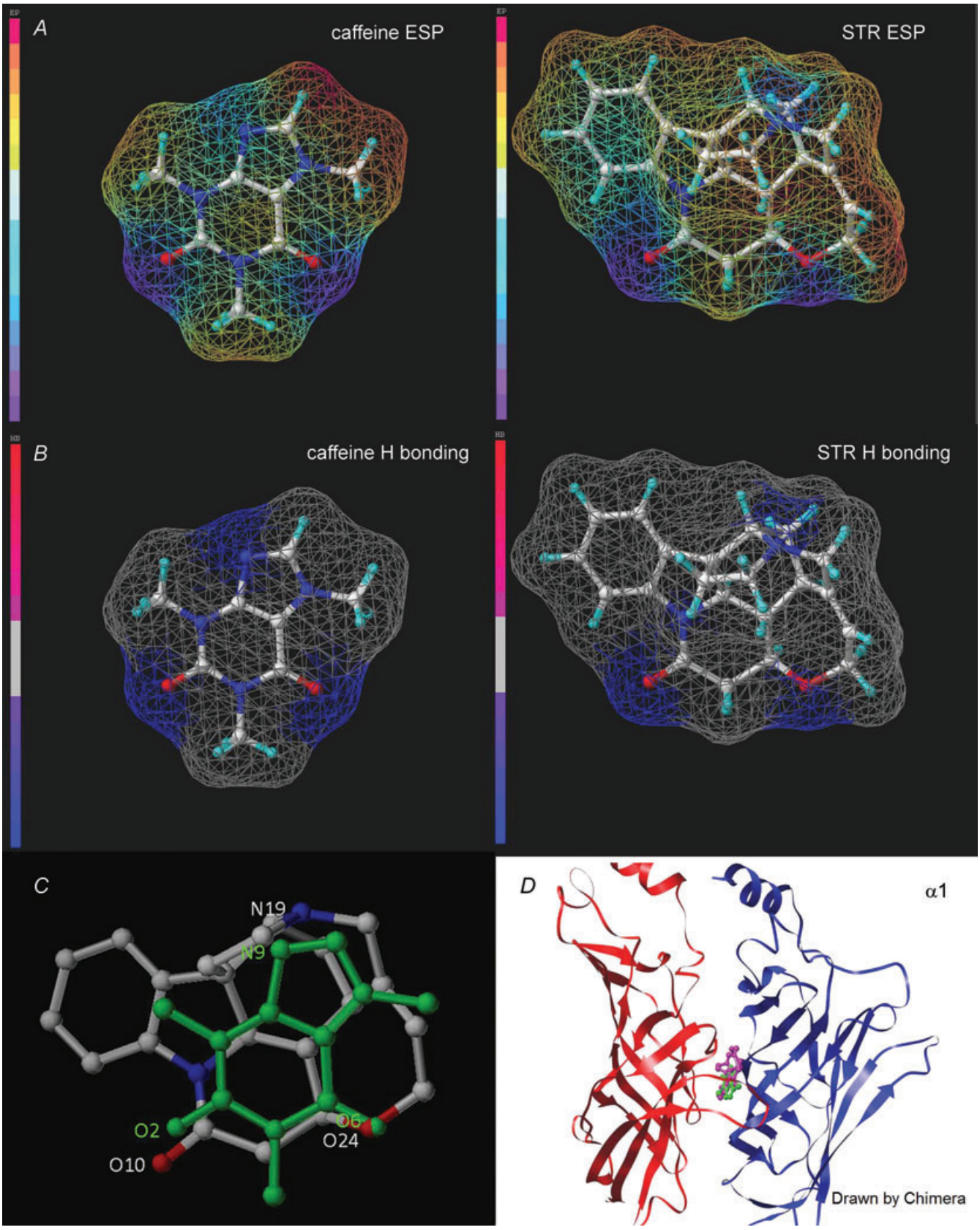

ganglion cell layer of the salamander retinal slice preparation, voltage clamped at 0 mV to isolate outward inhibitory currents. Glycine was applied at 100 μM, which produces a near-maximal (~92%) glycine current and is approximately 2.5 times the EC_{50} in amphibian retinal ganglion cells (Wang & Slaughter, 2005; Li & Slaughter, 2007). Glycine produced a large outward current that peaked and then partially desensitized (Fig. 1*A*). The glycine currents were suppressed by caffeine in a dose-dependent manner. There was nearly full inhibition at GlyRs at 10 mM caffeine, a concentration commonly used to activate ryanodine receptors. However, while 10 mM caffeine almost completely blocked the effect of 100 μM glycine, it did not suppress currents activated by 5 mM glycine (Fig. 1*B*), indicating that glycine and caffeine act competitively.

Using results such as that show in Fig. 1*A*, we generated inhibitory dose–response curves by fitting the data to the Hill equation (Fig. 1*C*). When tested against 100 μM glycine, caffeine inhibited the responses with an IC_{50} of about 1.7 mM and a Hill coefficient of 1.3 ($n = 9$).

Structural similarity between caffeine and strychnine

Strychnine is a potent competitive antagonist of glycine receptors, with an IC_{50} of 37 nM in amphibian retinal ganglion cells (Han *et al.* 1997).The strychnine molecule is quite complex and fairly bulky compared with glycine. However, caffeine and strychnine are similar in that they are multi-ring structures, are conformationally restricted, and have several moieties in common (Fig. 2*C*). Comparisons of the electrostatic (ESP) and hydrogen bonding profiles are shown in Fig. 2*A* and *B*, respectively, using SYBYL software (Tripos, see Methods). Both molecules have three electronegative (blue) atoms (upper panels) that are hydrogen acceptors (blue, lower panels). They are, respectively, O2, O6 and N9 on caffeine and O10, O24 and N19 on strychnine. The spatial arrangement of these three moieties is similar for the two molecules. In Fig. 2*C* the O6 of caffeine (green) and O24 of strychnine were superimposed, and the caffeine and strychnine were aligned to minimize the distanced of the other two moieties. Then the O2–O10 distance was 0.88 Å and the N9–N19 distance was 0.95 Å.

Other analogues of caffeine that contain the postulated three-site electrostatic profile of caffeine and strychnine also suppressed the glycine-induced current. Two examples are theophylline and theobromine (Fig. 1*D* and *E*). Compared to caffeine, theophylline and theobromine contain hydrogen instead of a methyl group on N7 or N1 of the xanthine ring, respectively. Whole cell currents were recorded from retinal slice ganglion cells exposed to 100 μM glycine in the presence or absence of 2 mM theophylline or 2 mM theobromine. Both suppressed responses to100 μM glycine.

Docking of caffeine and strychnine to α1 subunits of the GlyR

The electrostatic similarities between caffeine and strychnine suggested that caffeine may be able to bind the GlyR as strychnine does. To evaluate the potential interactions of caffeine at the GlyR, we performed a docking simulation of caffeine and strychnine at the α1 GlyR dimer. The model of the α1 subunit of the GlyR was obtained through homology modelling with the nAChR ligand binding domain (see Methods). An α1 dimer was formed using Chimera and then ligands were docked using Autodock. A docking simulation with strychnine yielded localization to the dimer interface that corresponded to that previously reported for the α1 subunit (Grudzinska *et al.* 2005; Speranskiy *et al.* 2007). The model in our simulation was more similar to Speranskiy *et al.* (2007) than to Grudzinska *et al.* (2005). When caffeine simulations were performed, the docking site was similar (Fig. 2*D*).

The α1 GlyR R159A mutation

If caffeine and strychnine share similar key binding sites and block through a similar mechanism, one might expect both molecules to be similarly affected by a putative binding site mutation. We examined a mutant that impaired the effectiveness of strychnine inhibition: the R131A mutation in α1 GlyRs greatly reduces strychnine binding without compromising receptor sensitivity to glycine (Grudzinska *et al.* 2005). This is a site in the

Figure 2. Structural similarities between caffeine and strychnine
A, electrostatic potentials (EPS) and *B*, hydrogen bonding maps of caffeine (left) and strychnine (right). Both molecules have three electronegative (blue) atoms (colour scale: red, most positive; purple, most negative) that are also hydrogen acceptors (colour scale: blue, high H acceptor density; red, high H donor density). *C*, alignment of caffeine (green) and strychnine (hydrogen atoms omitted) based on closest distance between three atom pairs (O2, O6, N9 on caffeine and O10, O24, N19 on strychnine). *D*, simulated docking of strychnine (blue) and caffeine (red) to an α1 dimer. The GlyR ligand binding domain model was obtained through homology modelling with nicotinic AChR ligand binding domain (see Methods). Using this model, caffeine and strychnine were docked to an overlapping binding region on the interface between two α1 subunits.

putative extracellular N-terminal region of the receptor. Strychnine directly interacts with R131 in the Grudzinska *et al.* model, but in our model the R131 is away from the strychnine and caffeine binding site and would act allosterically. The R131A α1 GlyR mutant was generated by site-directed mutagenesis of the rat α1 cDNA (see Methods), and expressed as homomers in HEK293 cells. Membrane currents were recorded in the presence of 60 μM glycine (EC_{50} for both the wild type and R131A α1 GlyRs) with different concentrations of caffeine (Fig. 3). Compared with the wild type α1 GlyR ($IC_{50} = 850 \pm 32$ μM, $n = 4$,), the efficacy of caffeine was reduced over 10-fold in the R131A mutant (IC_{50} of 9.7 ± 1.1 mM, $n = 7$). The shift in caffeine efficacy is similar but smaller than the reported 350-fold shift in strychnine efficacy (Grudzinska *et al.* 2005). This is supportive evidence that caffeine and strychnine have similar binding sites.

Caffeine's site of action is extracellular

The above results presume that caffeine is acting on the glycine receptor. However, caffeine as well as theobromine and theophylline can stimulate release of calcium from internal stores and can also inhibit phosphodiesterases. It is possible that caffeine modulation of intracellular pathways contributed to the inhibition of GlyRs. Therefore, experiments were designed to determine if caffeine was acting through an intracellular transduction mechanism or acting extracellularly on the glycine receptor.

At the concentrations used in this study, caffeine stimulates internal calcium release from the smooth endoplasmic reticulum via ryanodine receptors (reviewed in Zucchi & Ronca-Testoni, 1997).This mechanism underlies caffeine's suppression of $GABA_A$ receptor current on retinal ganglion cells (Akopian *et al.* 1998). To test whether glycine currents can be similarly modified by intracellular calcium levels, we used 10 μM ryanodine to elicit calcium release (Buck *et al.* 1992). The response of a retinal ganglion cell to 100 μM glycine was first determined. After recovery from glycine, the retinal slice was bathed in 10 μM ryanodine for 40 s followed by a second application of 100 μM glycine in the presence of 10 μM ryanodine. Ryanodine did not suppress the glycine current (Fig. 4*A*). To further test the possibility that internal calcium might play a role in caffeine's action, 10 mM BAPTA was placed inside the pipette solution in order to suppress a caffeine-induced increase in internal calcium. Retinal ganglion cells were then exposed to 100 μM glycine in the absence or presence of 10 mM caffeine. Caffeine produced full suppression of the glycine current in the presence of BAPTA (Fig. 4*B*).

Since caffeine can also increase cyclic nucleotide levels by inhibiting phosphodiesterase (Vurnikos-Danellis & Harris, 1968) we tested whether this may have an impact on glycine receptors. A potent phosphodiesterase inhibitor, IBMX (100 μM), was used to mimic caffeine's potential phosphodiesterase inhibition. IBMX did not significantly suppress the action of 100 μM glycine, indicating that caffeine did not act through this mechanism (Fig. 4*C*).

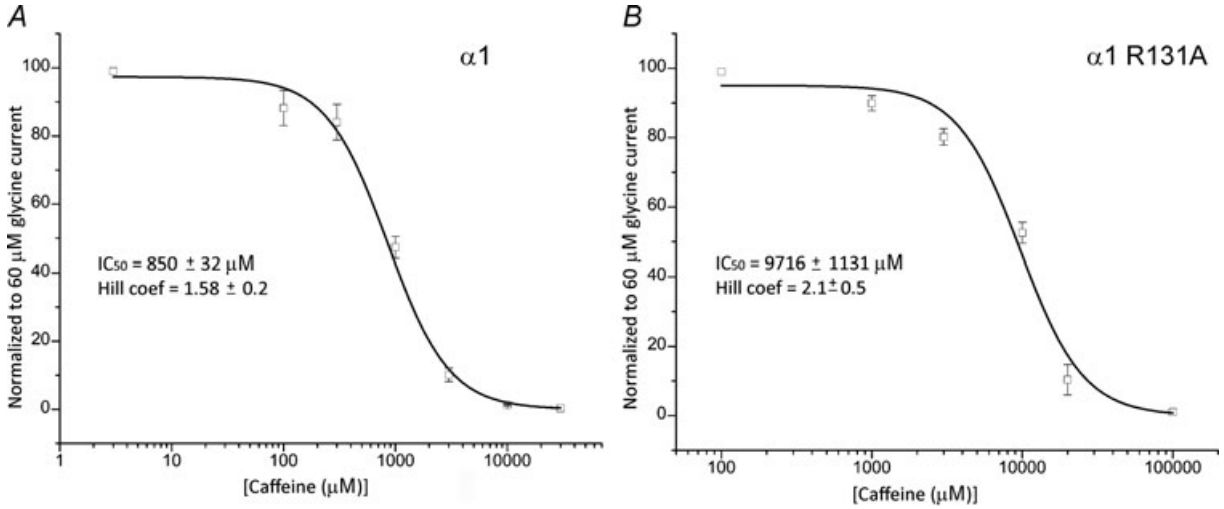

Figure 3. The R131A GlyR mutation decreases caffeine sensitivity of the α1 GlyR
HEK293 cells expressing rat homomeric wild type α1 (*A*) or mutant α1 R131A (*B*) GlyRs were held at −20 mV to record glycine-activated chloride currents. The cells were exposed to 60 μM (EC_{50}) glycine in the presence or absence of various concentrations of caffeine. The mutant GlyR ($n = 7$) caffeine IC_{50} was over 10 times higher than wild type ($n = 4$).

To further test if caffeine might be acting at an intracellular site to suppress GlyRs, we directly introduced caffeine to the cytoplasm by putting 10 mM caffeine in the pipette solution (Fig. 4*D*). The ganglion cells were then exposed to 100 μM glycine in the absence or presence of extracellularly applied 10 mM caffeine. As shown in Fig. 4*D*, left panel, intracellular caffeine did not eliminate glycine-activated current. More importantly, this current was still suppressed by extracellular 10 mM caffeine (middle panel), and this effect was reversible (right panel). Overall, these results indicate that caffeine acts at an extracellular membrane site to suppress the glycine current.

Antagonist properties of caffeine on α1β, α2β, α3β and α4β GlyR on HEK293 cells

To determine the relative sensitivity of glycine receptor subtypes, the action of caffeine was tested on each of the four α subunits, co-expressed with b subunits, in

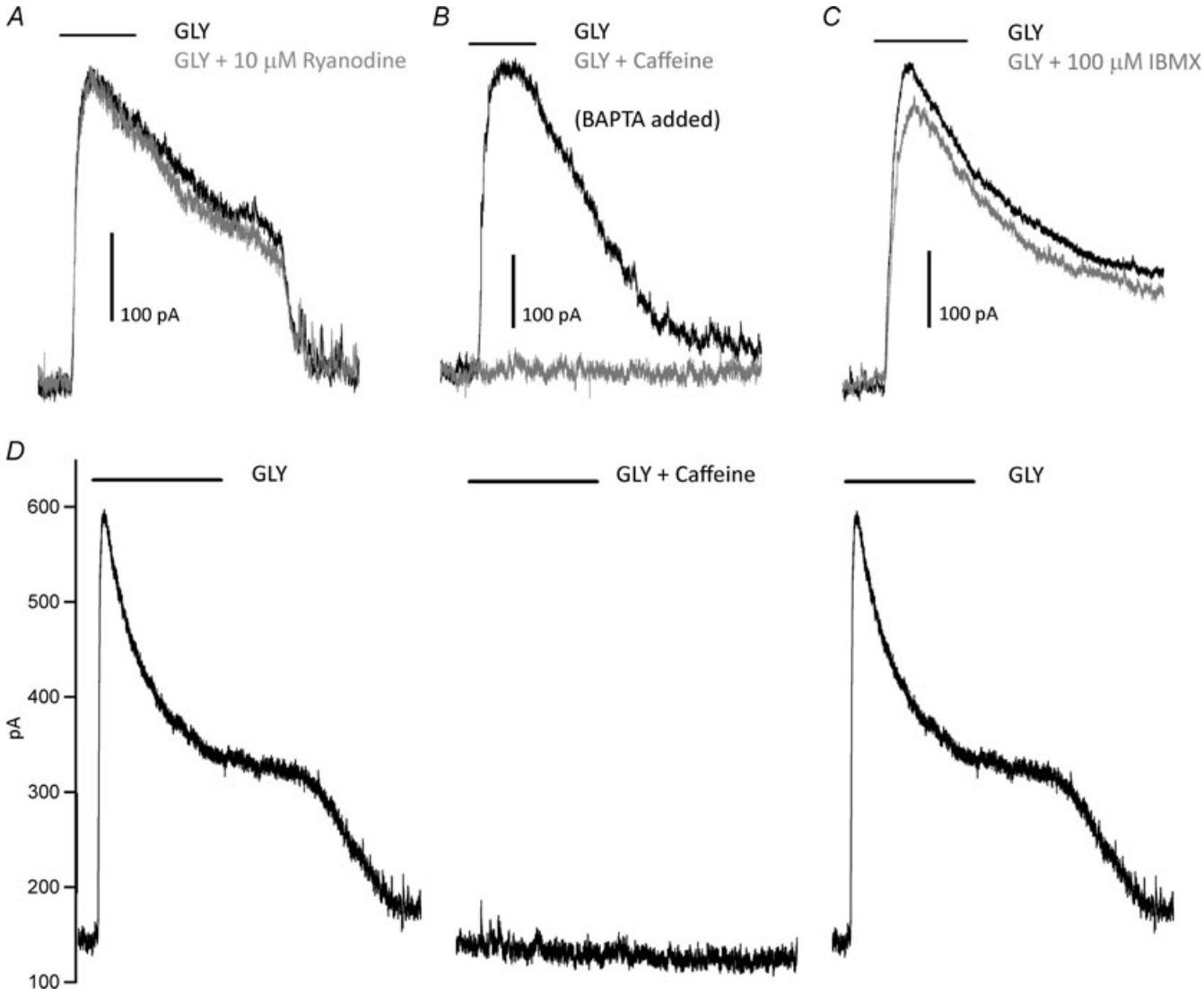

Figure 4. Caffeine blocks GlyRs at an extracellular site
Exogenous 100 μM glycine (indicated by bar above current trace)-activated currents recorded from retinal ganglion cells held at 0 mV. *A*, responses to glycine alone (black trace) or glycine in presence of 10 μM ryanodine (grey trace). Cells were pretreated with 10 μM ryanodine for 40 s before co-application with glycine. *B*, the pipette solution contained 10 mM BAPTA. After allowing several minutes for dialysis, neurons were exposed to glycine alone (black trace) or together with 10 mM caffeine (grey trace). *C*, currents elicited by glycine alone (black trace) or in the presence of 100 μM IBMX (grey trace). *D*, the pipette solution contained 10 mM caffeine. After several minutes of dialysis, neurons were exposed to glycine alone (left), together with 10 mM extracellular caffeine (middle), then glycine alone after removal of caffeine (right).

Table 1. Sensitivity of glycine receptor subunits to glycine and caffeine

	Glycine EC_{50} (μM)	Caffeine IC_{50} (μM)	EC_{50}/IC_{50} ratio
$\alpha1\beta$	60	837 ± 132	0.7
$\alpha2\beta$	100	248 ± 32	0.4
$\alpha3\beta$	340	255 ± 16	1.33
$\alpha4\beta$	70	517 ± 50	0.14

The table shows the glycine EC_{50} and caffeine IC_{50} (against the EC_{50} glycine concentration) values for the GlyR heteromers expressed in HEK293 cells. The EC_{50}/IC_{50} ratio provides a metric for comparing caffeine block at receptors with differing glycine efficacies. A higher ratio indicates a more effective block by caffeine.

HEK293 cells (Fig. 5). Native GlyRs are believed to be predominantly $\alpha\beta$ heteromers (Grudzinska *et al.* 2005). The efficacy of glycine is very different among the four GlyR subtypes, so to compare caffeine potency we used the EC_{50} of glycine at each of the four receptors (Table 1). Caffeine suppressed $\alpha2\beta$ (IC_{50} of 248 ± 32 μM against 100 μM glycine, $n = 7$) and $\alpha3\beta$ (IC_{50} of 255 ± 16 μM against 340 μM glycine, $n = 7$) most potently. The $\alpha1\beta$ GlyR was the most difficult to block (IC_{50} of 837 ± 132 μM against 60 μM glycine, $n = 8$). On the $\alpha4\beta$ GlyR, caffeine's IC_{50} was 517 ± 50 μM against 70 μM glycine ($n = 10$). Thus, caffeine blocked the various GlyRs subtypes with about a 3-fold range in effectiveness (summarized in Table 1).

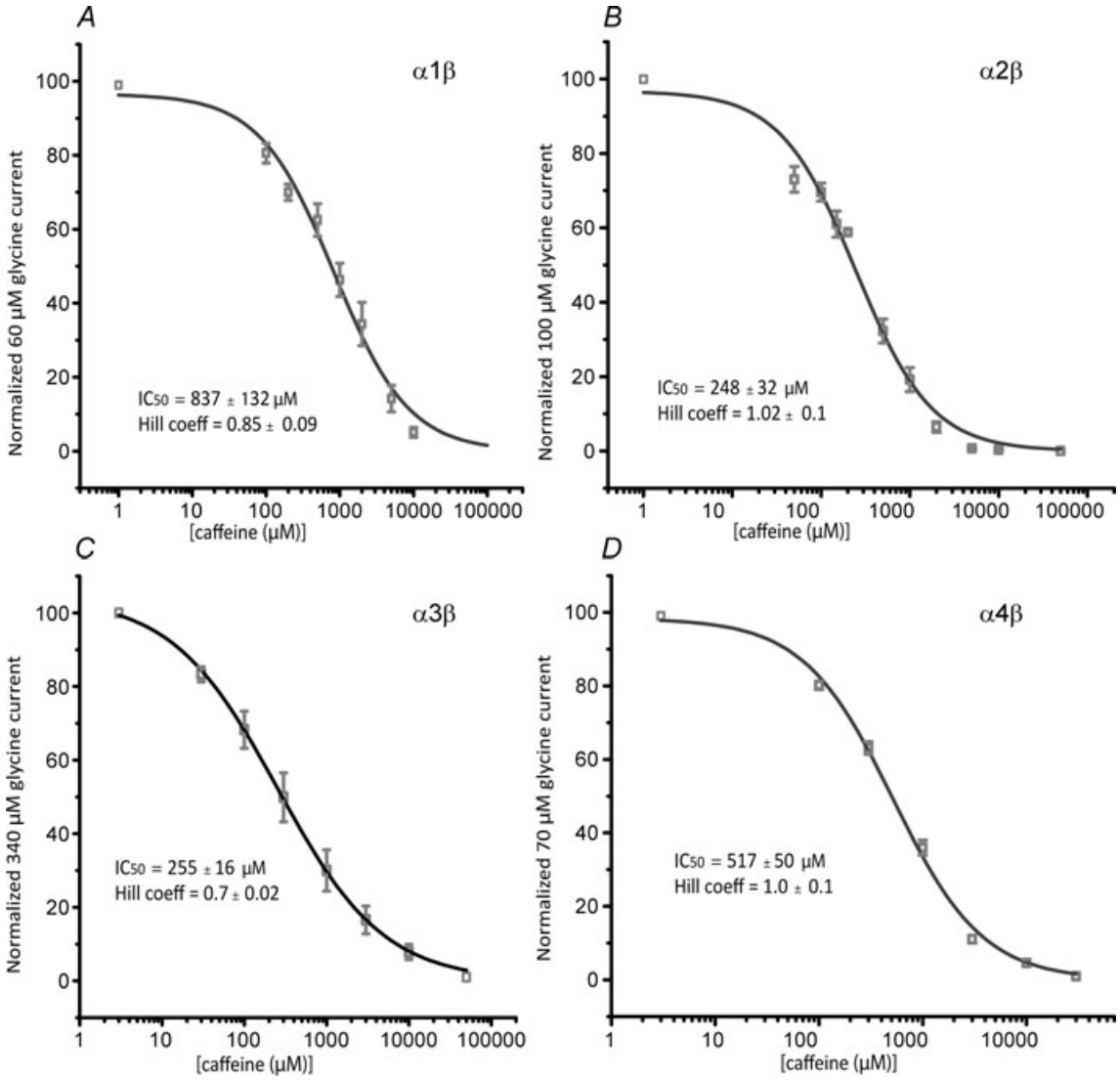

Figure 5. Caffeine inhibition of GlyR subtypes
HEK293 cells expressing rat heteromeric $\alpha\beta$ GlyRs were held at −20 mV to record chloride currents. The effects of various concentrations of caffeine were tested against the EC_{50} concentration of glycine for each GlyR subtype: *A*, 60 μM glycine for $\alpha1\beta$ ($n = 8$); *B*, 100 μM glycine for $\alpha2\beta$ ($n = 7$); *C*, 340 μM glycine for $\alpha3\beta$ ($n = 7$); and *D*, 70 μM glycine for $\alpha4\beta$ ($n = 10$). Data were fitted to the Hill equation (see Methods).

However, if both the EC_{50} and IC_{50} values are considered, then for a given absolute level of glycine the $\alpha3\beta$ GlyR is relatively easy to block while the $\alpha1\beta$ GlyR is particularly difficult to block with caffeine. This is reflected in the EC_{50}/IC_{50} ratios for the four receptors: 0.07, 0.40, 1.33 and 0.14 for $\alpha1\beta$, $\alpha2\beta$, $\alpha3\beta$ and $\alpha4\beta$, respectively (Table 1).

Caffeine shifts the glycine dose–response curve of $\alpha3\beta$ GlyR

The above experiments indicate that caffeine is a particularly effective antagonist at the $\alpha3\beta$ GlyRs. To explore this we tested the effect of 300 μM caffeine on the glycine dose–response of the $\alpha3\beta$ GlyR expressed in HEK293 cells (Fig. 6). This relatively low dose of caffeine shifted the glycine EC_{50} from 338 μM to 497 μM. High concentrations of glycine could overcome the block, indicative of competitive inhibition.

Caffeine effect on glycinergic synaptic transmission

If caffeine inhibits GlyRs, then it should reduce post-synaptic responses in retinal ganglion cells because they receive a significant input from glycinergic amacrine cells. Ganglion cells in the retinal slice preparation were held at 0 mV and recorded under dark-adapted conditions, thereby monitoring both spontaneous and light-evoked inhibitory currents. Glycinergic IPSCs were isolated by blocking GABAergic inputs with SR95531 (5 μM). As shown in Fig. 7, there was a dose-dependent suppression of both spontaneous and light-evoked currents by caffeine. The sensitivity to caffeine varied slightly from cell to cell, but two patterns of inhibition were apparent. In the cell shown in Fig. 7*A*, 2 mM caffeine almost completely suppressed glycinergic IPSCs, both spontaneous and light-evoked. However, in the cell depicted in Fig. 7*B*, a few spontaneous events were still evident in 2 mM caffeine and light-evoked IPSCs were detectable in the presence of 5 mM caffeine, although most spontaneous events were eliminated. This variability may reflect caffeine sensitivity differences between GlyR subtypes. However, as argued below, this is not a likely explanation. The difference in caffeine sensitivity between spontaneous and light-evoked IPSCs in the second cell suggests that the glycine concentration at the synapse was elevated during stimulated release compared to spontaneous release. In the first cell, the similar caffeine sensitivity of spontaneous and light-evoked currents seems to indicate that the light-evoked response involves the synchronization of more synapses but not an elevation of glycine concentration at each synapse.

To evaluate the nature of caffeine suppression at the synapse, we analysed spontaneous glycinergic IPSCs in the presence or absence of 500 μM caffeine. Spontaneous IPSCs were recorded from ganglion cells while the retina was held in the dark. The amplitude of each spontaneous event and the time between spontaneous events were measured. To evaluate this type of data, the suppressive effects of caffeine had to be small to avoid missed events. Thus, we selected neurons in which the effects of 500 μM caffeine were small (such as events observed in Fig. 7*B* rather than 7*A*). The cumulative distribution of amplitudes and inter-event intervals under control conditions and in the presence of 500 μM caffeine are shown for one such retinal ganglion cell (Fig. 7*C* and *D*). Caffeine shifted the amplitude distribution to the left and had little effect on the inter-event interval. Similar findings were observed on three other ganglion cells. This result is consistent with a caffeine block of post-synaptic receptors without altering release properties of glycinergic amacrine cells. It is likely that higher doses of caffeine might affect release as well because internal calcium stores can influence this process (Warrier *et al.* 2005; Suryanarayanan & Slaughter, 2006).

Caffeine effect on light-evoked and spontaneous synaptic events

The effect of various doses of caffeine on light-evoked glycinergic IPSCs was measured in ganglion cells. The peak IPSC amplitude *vs.* caffeine concentration was fitted to the Hill equation yielding an IC_{50} of 1.65 ± 0.22 mM and a Hill coefficient of 1.3 ± 0.2 (Fig. 7*E*, $n = 11$). Curiously, this dose–response curve closely matched caffeine inhibition of exogenous application of 100 μM glycine (Fig. 1*C*). However, Fig. 1*C* represents a steady state inhibition while Fig. 7*E* represents a non-steady state block of a transient increase of glycine. Thus, at the synapse the effect

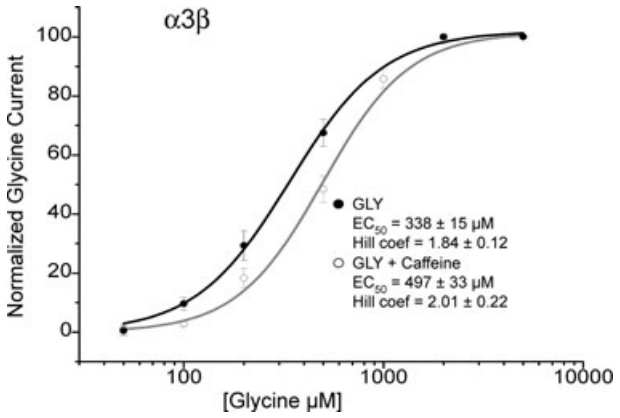

Figure 6. Caffeine inhibits glycine responses in $\alpha3\beta$ GlyRs
Various concentrations of glycine with or without 300 μM caffeine were applied to HEK293 cells expressing $\alpha3\beta$ GlyRs. The glycine EC_{50} concentration was increased from 338 ± 15 μM ($n = 9$) to 497 ± 33 by 300 μM caffeine ($n = 9$).

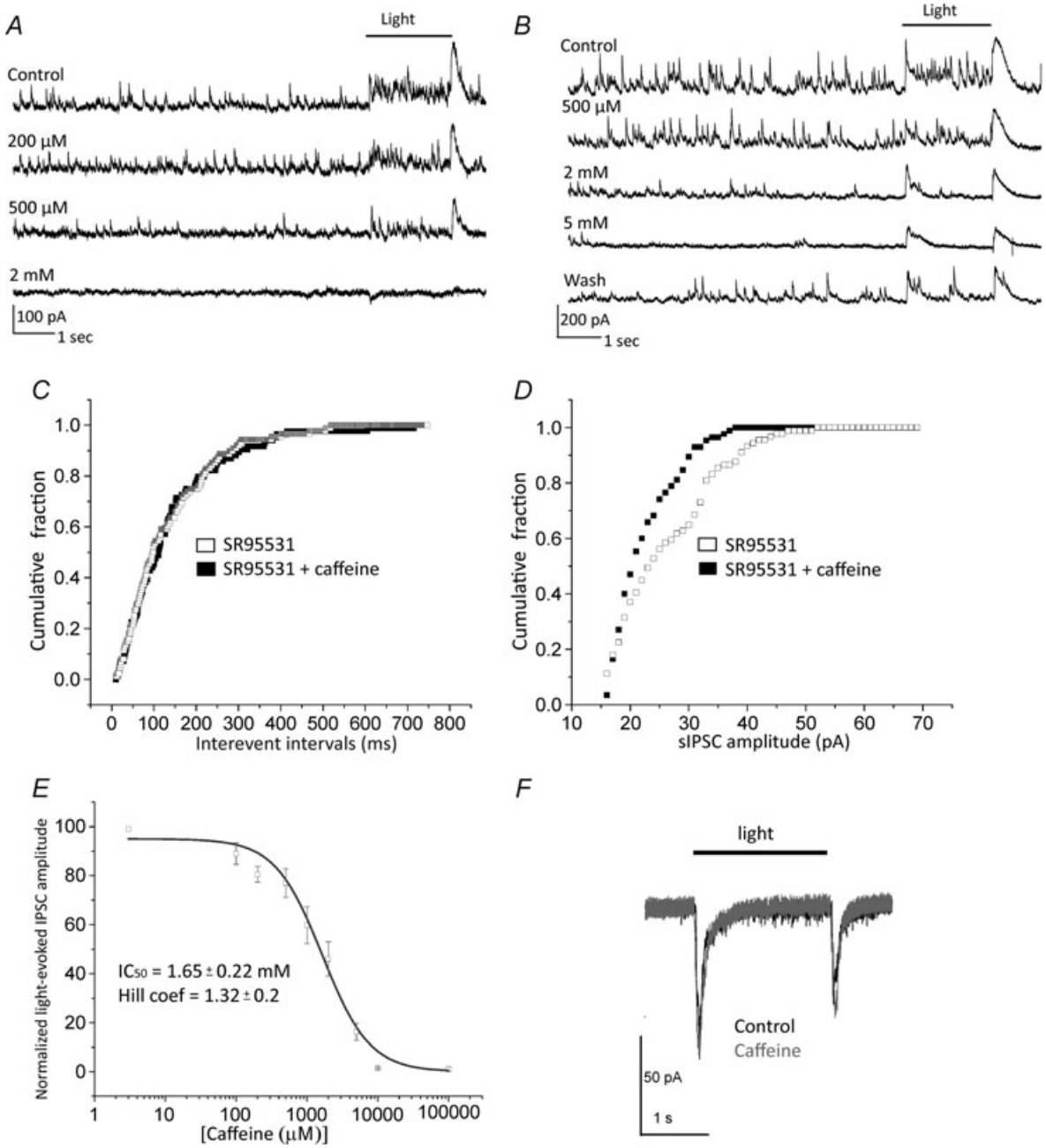

Figure 7. Caffeine suppression of spontaneous and light-evoked glycinergic IPSCs on retinal ganglion cells

Retinal ganglion cells were held at 0 mV to record IPSCs. GABAergic inputs were blocked by SR95531 (5 μM). *A*, decreases in amplitude of both spontaneous IPSCs and light-evoked IPSCs were noted in the presence of 200 μM caffeine. 2 mM caffeine completely suppressed all glycinergic IPSCs. *B*, 5 mM caffeine blocked spontaneous but not light-evoked IPSCs. *C* and *D*, spontaneous glycinergic IPSCs were measured before and during the application of 500 μM caffeine. *C*, caffeine did not alter the inter-event interval between spontaneous events. *D*, caffeine did reduce the amplitude of spontaneous events. *E*, a dose–response curve showing the effect of various caffeine concentrations on the peak light-evoked glycinergic IPSCs recorded in ganglion cells. Cells were held at 0 mV and GABAergic responses were blocked with 5 μM SR95531. A Hill plot to the data yielded a caffeine IC_{50} of 1.65 ± 0.22 mM ($n = 12$). *F*, a ganglion cell was held at -70 mV to isolate the light-evoked EPSC and 50 μM picrotoxinin and 10 μM strychnine were co-applied to eliminate inhibitory currents. Light-evoked EPSCs were recorded in the absence (black trace) or presence of 10 mM caffeine (grey trace).

of caffeine includes an added component: the time for dissociation of pre-applied caffeine from the receptor. Therefore, the similarity of these values is probably coincidental. However, even though caffeine inhibition can be overcome by high glycine concentrations, as assumed to exist at the synapse, caffeine is an effective antagonist of synaptic glycine.

The present studies indicate that caffeine can inhibit glycinergic IPSCs and previous work indicated that caffeine can suppress GABAergic IPSCs in retina (Akopian *et al.* 1998). Does caffeine also affect excitatory glutamatergic input to retinal ganglion cells? Retinal ganglion cells were held at −70 mV so that excitatory currents would be recorded as inward currents. Figure 7*F* shows that there is no change in amplitude of light-evoked EPSCs in the presence of 10 mM caffeine. This concentration of caffeine also failed to modify currents activated by exogenous 100 μM glutamate in retinal ganglion cells (data not shown).

Discussion

Caffeine and strychnine

These experiments indicate that glycine receptors can be inhibited by caffeine. This suppression seems to be through direct binding of caffeine to the GlyR and the site of binding may be similar for both caffeine and strychnine. Caffeine and strychnine both have a set of three electronegative atoms that can be approximately aligned. Docking simulations and site-directed mutagenesis both support the hypothesis that caffeine and strychnine bind to similar sites on the receptor. Unlike strychnine, whose structure is complex, caffeine is a flat, two-ringed, conformationally restricted molecule. Consequently, it is simpler to identify the key moieties in caffeine that interact with the receptor and it may prove to be a model for the design of future glycine receptor antagonists. The same three charged groups on strychnine were identified as potential binding moieties in the docking simulations performed by Grudzinska *et al.* (2005). The three charged moieties in both antagonists replicate the charges of glycine, although glycine cannot match the distances between the moieties. This separation may explain the competitive antagonism, whereby the antagonists stabilize the subunits at a distance that does not lead to gating. Caffeine is far less potent than strychnine and the three moieties clearly do not superimpose on the two molecules. Whether this accounts for the difference in potency, or whether other components of strychnine are also important in receptor inhibition, is unresolved.

Glycine receptor subtypes in amphibian retina

The effects of glycine and caffeine lead to several conclusions, with the caveats that correlations are being made between rat glycine receptors expressed in HEK293 cells and retinal glycine receptors in amphibians. If analogies can be derived from these two systems, then it would suggest that the synaptic responses in third order neurons are dominated by activation of $\alpha1\beta$ GlyRs while the $\alpha3\beta$ GlyR makes little contribution. This is based on two sets of data. One is that the native glycine receptor has an EC_{50} of 40 μM and a Hill coefficient that exceeds 2 (Wang & Slaughter, 2005). The steep Hill coefficient indicates that the response is produced by one set of receptors or a set of receptors that have EC_{50}s that are very similar. Among the four subytpes of GlyR, the $\alpha2\beta$ has an EC_{50} of 100 μM and the $\alpha3\beta$ EC_{50} is 340 μM; neither is likely to produce the response seen in retinal ganglion cells. The $\alpha1\beta$ and $\alpha4\beta$ GlyRs have EC_{50}s of 60 μM and 70 μM, respectively, making them more likely candidates. The second point is the observation that caffeine's IC_{50} is 1.65 mM in response to 100 μM exogenous glycine in amphibian ganglion cells. Again, this is inconsistent with the properties of $\alpha2\beta$ or $\alpha3\beta$ GlyRs, both of which exhibit much more inhibition to those doses. The $\alpha1\beta$ GlyR has the least sensitivity to caffeine and would have a caffeine IC_{50} near 1.6 mM in response to 100 μM glycine. It is surprising that more receptor subtypes are not expressed in amphibian ganglion cells, but the conclusion is consistent with the steep glycine dose–response curve reported previously (Wang & Slaughter, 2005; Li & Slaughter 2007) and the sharp caffeine dose–response curve reported here. In rat retinal ganglion cells the glycine dose–response curve is more shallow, due to the presence of $\alpha3\beta$ receptors (Majumdar *et al.* 2007; A Neelakantan & MM Slaughter, personal communications).

A similar predominance of $\alpha1\beta$ GlyRs was found in the large, A-type ganglion cells in mouse retina. Majumdar *et al.* (2007) found spontaneous glycinergic IPSCs in these neurons with the fast kinetics typical of $\alpha1\beta$ GlyRs. In GlyR $\alpha1$ knockouts the average event was slower, but in GlyR $\alpha2$ or $\alpha3$ knockouts the events were essentially unaffected. However, sIPSCs with slower kinetics are evident in other ganglion cells (Protti *et al.* 1997), indicating synaptic GlyRs are not limited to $\alpha1\beta$. It is possible that we were selecting from a subset of amphibian ganglion cells, although we did choose neurons with various somata shapes and sizes.

Glycinergic synaptic currents

Caffeine suppressed glycinergic spontaneous and light-evoked synaptic events. Comparing the effect of caffeine on these events revealed two phenomena. In one set of neurons, the spontaneous events and light-evoked IPSCs were both fully suppressed at similar concentrations of caffeine (e.g. Fig. 5*A*). In other neurons, the spontaneous events were eliminated at lower caffeine concentrations than the evoked events. If these different responses are not due to different subtypes of GlyR, as

argued above, then it indicates that in some neurons light-evoked responses are simply summed discrete synaptic events, while in other neurons the light-evoked event results from elevated levels of glycine at the synapse.

Summary

Caffeine is a weak competitive antagonist of glycine receptors, which exhibits a slight preference for the $\alpha 2$ and $\alpha 3$ GlyRs. Like a few other weak antagonists, such as picrotoxin and 2,4 dichlorokynurenic acid, the $\alpha 1$ GlyR is less susceptible to block (Wang & Slaughter, 2005; Han *et al.* 1997). One interesting feature of caffeine is that it is a flat and conformationally restricted molecule that may aid in structure–function analysis.

References

Akopian A, Gabriel R & Witkovsky P (1998). Calcium released from intracellular stores inhibits $GABA_A$-mediated currents in ganglion cells of the turtle retina. *J Neurophysiol* **80**, 1105–1115.

Arnold K, Bordoli L, Kopp J & Schwede T (2006). The SWISS-MODEL workspace: a web-based environment for protein structure homology modelling. *Bioinformatics* **22**, 195–201.

Awatramani G, Wang J & Slaughter MM (2001). Amacrine and ganglion cell contributions to the electroretinogram in amphibian retina. *Vis Neurosci* **18**, 147–156.

Buck E, Zimanyi I, Abramson JJ & Pessah IN (1992). Ryanodine stabilizes multiple conformational states of the skeletal muscle calcium release channel. *J Biol Chem* **267**, 23560–23567.

Enz R & Bormann J (1995). Expression of glycine receptor subunits and gephyrin in single bipolar cells of the rat retina. *Vis Neurosci* **12**, 501–507.

Gisselmann G, Galler A, Friedrich F, Hatt H & Bormann J (2002). Cloning and functional characterization of two glycine receptor α-subunits from the perch retina. *Eur J Neurosci* **16**, 69–80.

Greferath U, Brandstatter JH, Wassle H, Kirsch J, Kuhse J & Grunert U (1994). Differential expression of glycine receptor subunits in the retina of the rat: a study using immunohistochemistry and in situ hybridization. *Vis Neurosci* **11**, 721–729.

Grudzinska J, Schemm R, Haeger S, Nicke A, Schmalzing G, Betz H & Laube B (2005). The β subunit determines the ligand binding properties of synaptic glycine receptors. *Neuron* **45**, 727–739.

Grunert U & Wassle H (1996). Glycine receptors in the rod pathway of the macaque monkey retina. *Vis Neurosci* **13**, 101–115.

Guex N & Peitsch MC (1997). SWISS-MODEL and the Swiss-PdbViewer: an environment for comparative protein modeling. *Electrophoresis* **18**, 2714–2723.

Han Y, Li P & Slaughter MM (2004). Selective antagonism of rat inhibitory glycine receptor subunits. *J Physiol* **554**, 649–658.

Han Y, Zhang J & Slaughter MM (1997). Partition of transient and sustained inhibitory glycinergic input to retinal ganglion cells. *J Neurosci* **17**, 3392–3400.

Haverkamp S, Muller U, Harvey K, Harvey RJ, Betz H & Wassle H (2003). Diversity of glycine receptors in the mouse retina: localization of the $\alpha 3$ subunit. *J Comp Neurol* **465**, 524–539.

Haverkamp S, Muller U, Zeilhofer HU, Harvey RJ & Wassle H (2004). Diversity of glycine receptors in the mouse retina: localization of the $\alpha 2$ subunit. *J Comp Neurol* **477**, 399–411.

Heinze L, Harvey RJ, Haverkamp S & Wassle H (2007). Diversity of glycine receptors in the mouse retina: localization of the $\alpha 4$ subunit. *J Comp Neurol* **500**, 693–707.

Ivanova E, Muller U & Wassle H (2006). Characterization of the glycinergic input to bipolar cells of the mouse retina. *Eur J Neurosci* **23**, 350–364.

Jusuf PR, Haverkamp S & Grunert U (2005). Localization of glycine receptor α subunits on bipolar and amacrine cells in primate retina. *J Comp Neurol* **488**, 113–128.

Kneussel M & Betz H (2000). Clustering of inhibitory neurotransmitter receptors at developing postsynaptic sites: the membrane activation model. *Trends Neurosci* **23**, 429–435.

Laube B, Maksay G, Schemm R & Betz H (2002). Modulation of glycine receptor function: a novel approach for therapeutic intervention at inhibitory synapses? *Trends Pharmacol Sci* **23**, 519–527.

Li P & Slaughter M (2007). Glycine receptor subunit composition alters the action of GABA antagonists. *Vis Neurosci* **24**, 513–521.

Majumdar S, Heinze L, Haverkamp S, Ivanova E & Wassle H (2007). Glycine receptors of A-type ganglion cells of the mouse retina. *Vis Neurosci* **24**, 471–487.

Marvizon JC, Vazquez J, Garcia Calvo M, Mayor F Jr, Ruiz Gomez A, Valdivieso F & Benavides J (1986). The glycine receptor: pharmacological studies and mathematical modeling of the allosteric interaction between the glycine- and strychnine-binding sites. *Mol Pharmacol* **30**, 590–597.

Matzenbach B, Maulet Y, Sefton L, Courtier B, Avner P, Guenet JL & Betz H (1994). Structural analysis of mouse glycine receptor α subunit genes. Identification and chromosomal localization of a novel variant. *J Biol Chem* **269**, 2607–2612.

Meyer G, Kirsch J, Betz H & Langosch D (1995). Identification of a gephyrin binding motif on the glycine receptor β subunit. *Neuron* **15**, 563–572.

Pettersen EF, Goddard TD, Huang CC, Couch GS, Greenblatt DM, Meng EC & Ferrin TE (2004). UCSF chimera – a visualization system for exploratory research and analysis. *J Comput Chem* **25**, 1605–1612.

Pribilla I, Takagi T, Langosch D, Bormann J & Betz H (1992). The atypical M2 segment of the β subunit confers picrotoxinin resistance to inhibitory glycine receptor channels. *EMBO J* **11**, 4305–4311.

Protti DA, Gerschenfeld HM & Llano I (1997). GABAergic and glycinergic IPSCs in ganglion cells of rat retinal slices. *J Neurosci* **17**, 6075–6085.

Rajendra S & Schofield PR (1995). Molecular mechanisms of inherited startle syndromes. *Trends Neurosci* **18**, 80–82.

Ruiz-Gomez A, Morato E, Garcia-Calvo M, Valdivieso F & Mayor F Jr (1990). Localization of the strychnine binding site on the 48-kilodalton subunit of the glycine receptor. *Biochemistry* **29**, 7033–7040.

Sassoe-Pognetto M & Wassle H (1997). Synaptogenesis in the rat retina: subcellular localization of glycine receptors, $GABA_A$ receptors, and the anchoring protein gephyrin. *J Comp Neurol* **381**, 158–174.

Smiley JF & Yazulla S (1990). Glycinergic contacts in the outer plexiform layer of the *Xenopus laevis* retina characterized by antibodies to glycine, GABA and glycine receptors. *J Comp Neurol* **299**, 375–388.

Speranskiy K, Cascio M & Kurnikova M (2007). Homology modeling and molecular dynamics simulations of the glycine receptor ligand binding domain. *Proteins* **67**, 950–960.

Suryanarayanan A & Slaughter MM (2006). Synaptic transmission mediated by internal calcium stores in rod photoreceptors. *J Neurosci* **26**, 1759–1766.

Vernikos-Danellis N & Harris CG (1968). The effect of *in vitro* and *in vivo* caffeine, theophylline, and hydrocortisone on the phosphodiesterase activity of the pituitary, mdian eminence, hem, and cerebral conex of the rat. *Proc Soc Exp Biol Med* **128**(4), 1016–1021.

Wang P & Slaughter MM (2005). Effects of GABA receptor antagonists on retinal glycine receptors and on homomeric glycine receptor a subunits. *J Neurophysiol* **93**, 3120–3126.

Warrier A, Borges S, Dalcino D, Walters C & Wilson M (2005). Calcium from internal stores triggers GABA release from retinal amacrine cells. *J Neurophysiol* **94**, 4196–4208.

Wassle H (2004). Parallel processing in the mammalian retina. *Nat Rev Neurosci* **5**, 747–757.

Young AB & Snyder SH (1973). Strychnine binding associated with glycine receptors of the central nervous system. *Proc Natl Acad Sci U S A* **70**, 2832–2836.

Zucchi R & Ronca-Testoni S (1997). The sarcoplasmic reticulum Ca^{2+} channel/ryanodine receptor: modulation by endogenous effectors, drugs and disease states. *Pharmacol Rev* **49**, 1–51.

Author contributions

Lei Duan, Jaeyoung Yang and Malcolm Slaughter were all involved in the conception, design and analysis of the data. All three participated in drafting the manuscript and will participate in the final approval of the version to be published.

Acknowledgements

This work was supported by National Eye Institute grants EY 05725 and EY14960. We thank Jason Myers for preparing the R131A GlyR mutant.